# Supporting Information

## Charge Transfer Modulation in Layer-by-Layer-Assembled Multilayered Photoanodes for Solar Water Oxidation

Shuo Hou,[a] Xiao-Cheng Dai,[a] Yu-Bing Li,[a] Ming-Hui Huang,[a] Tao Li,[a] Zhi-Quan Wei,[a] Yunhui He,[b] Guangcan Xiao,[b] Fang-Xing Xiao[a]*

a. College of Materials Science and Engineering, Fuzhou University, New Campus, Minhou, Fujian Province 350108, China.

b. Instrumental Measurement and Analysis Center, Fuzhou University, Fuzhou, 350002, People's Republic of China.

E-mail: fxxiao@fzu.edu.cn

## 1. Preparation of negatively charged CdS QDs

Briefly, 250 μL of mercaptoacetic acid (MMA) was added to 50 mL of $CdCl_2$ (10 mM) aqueous solution, and $N_2$ was bubbled throughout the solution to remove $O_2$ at 110 °C. During this period, 1.0 M NaOH aqueous solution was slowly added to adjust the solution pH to 11. Following, 5.5 mL of 0.1 M $Na_2S$ aqueous solution was injected to grow the MMA-capped water-soluble CdS QDs. The reaction mixture was refluxed under $N_2$ atmosphere for 4 h. Finally, the desired MMA-stabilized CdS QDs were synthesized and stored in a refrigerator at 4 °C for further use. [S1]

## 2. Preparation of negatively charged CdTe QDs

CdTe QDs were synthesized by an aqueous synthesis method reported previously with some modifications. Specifically, 2 mmol of $CdCl_2 \cdot 2.5H_2O$ was dissolved in 200 mL of DI $H_2O$ and deaerated with $N_2$ bubbling in a three-necked flask for 1 h. After that, 230 μL of MAA as a stabilizer was added into the above solution and pH value of the mixture was carefully adjusted to 11 with 1 M NaOH aqueous solution. Subsequently, oxygen-free NaHTe aqueous solution was prepared by dissolving 1.2640 g of $NaBH_4$ in 10 mL of DI $H_2O$ under $N_2$ bubbling, into which 0.3403 g of Te powder was added and stirred at a low speed for 2 h in an ice bath. 5 mL of the freshly prepared NaHTe aqueous solution was then quickly injected into $Cd^{2+}$ aqueous solution under vigorous stirring and a red solution was obtained and then it was refluxed in 333 K for 4 h. After cooling to room temperature, CdTe QDs aqueous solution was precipitated by adding into equal volume of ethanol with vigorous stirring and the precipitate was separated by centrifugation and dried in vacuum at 313 K.[S2]

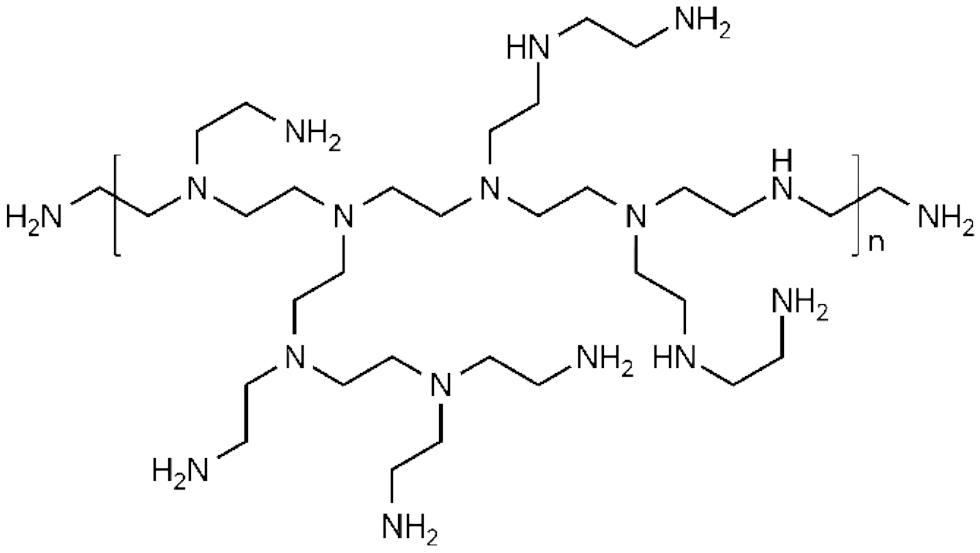


**Fig. S1.** Molecular structure of BPEI.

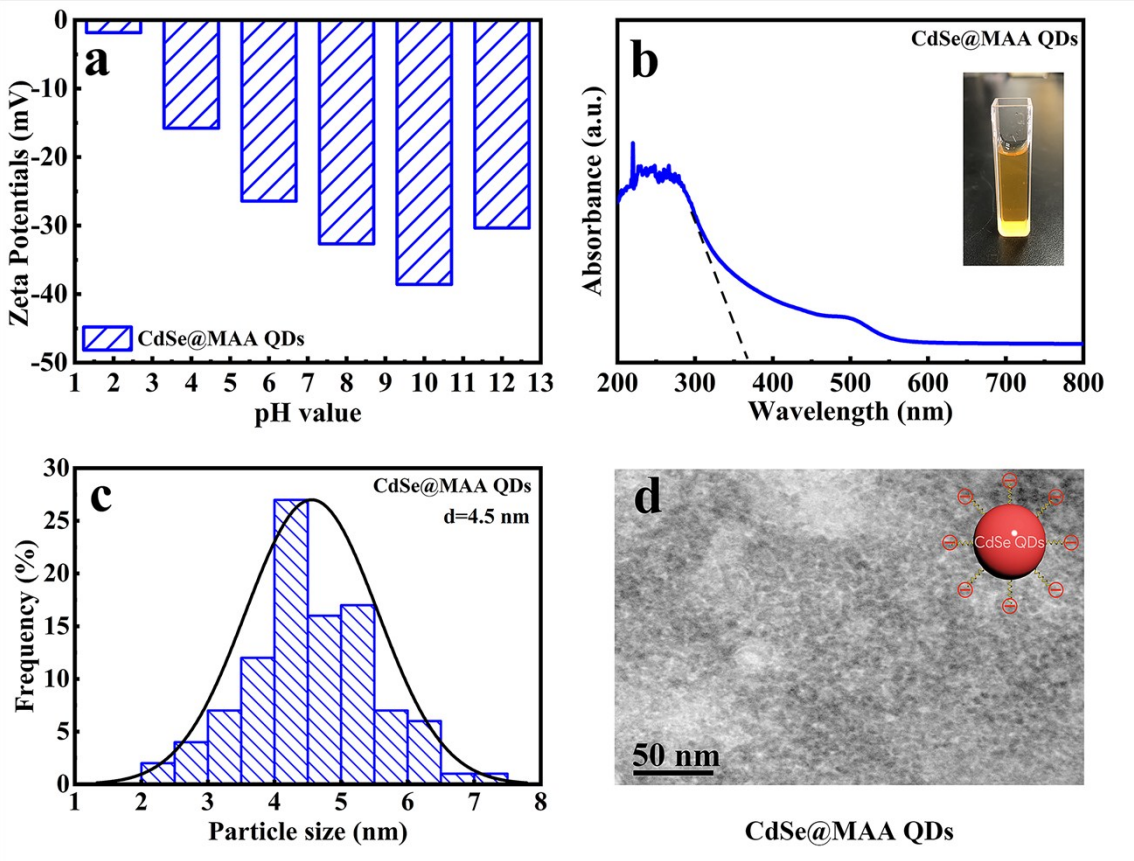


**Fig. S2.** (a) Zeta potential, (b) UV-vis adsorption spectrum, (c) size distribution histogram and (d) TEM image of CdSe@MAA QDs with schematic model in the inset.

**Table. S1** Peak position with corresponding functional groups for CdSe@MAA QDs and $T(BC)_4$.

| *Peak position ($cm^{-1}$)* | *Functional Groups* |
|---|---|
| **3443.9** | -OH |
| **2924** | $-CH_2-$ |
| **2846** | $-CH_2-$ |
| **1628** | $-COO^-$ |
| **1415** | Ti-O |
| **1115** | Ti-O |

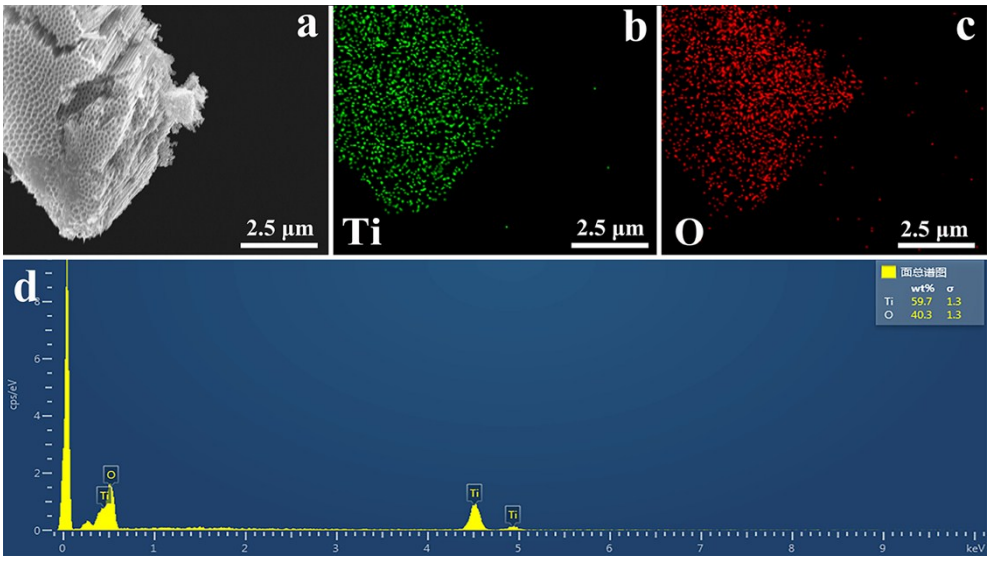


**Fig. S3.** NP-TNTAs with corresponding EDS and elemental mapping result.

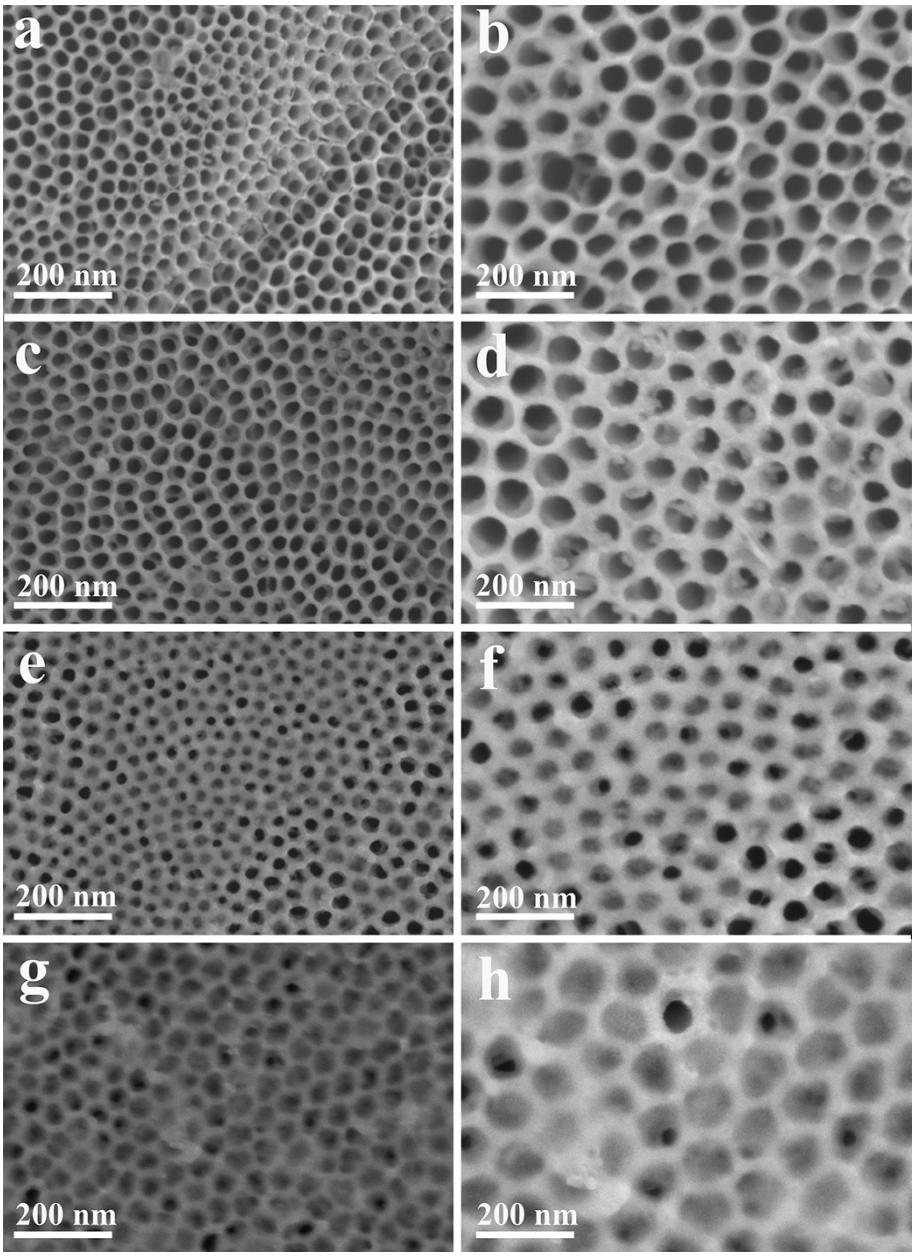


**Fig. S4.** Panoramic FESEM images of (a & b) $T(BC)_1$, (c & d) $T(BC)_2$, (e & f) $T(BC)_6$, and (g & h) $T(BC)_8$ multilayered heterostructures with different assembly bilayer.

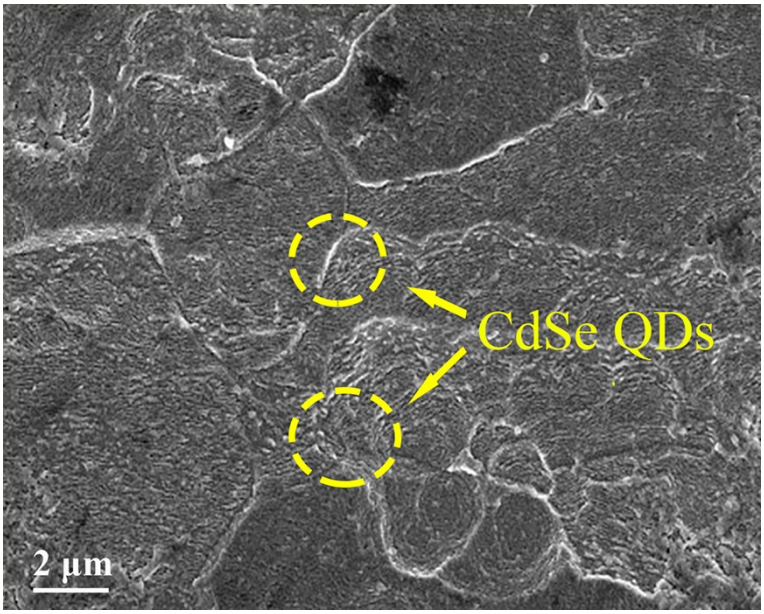


**Fig. S5.** FESEM image of $Ti(BC)_4$.

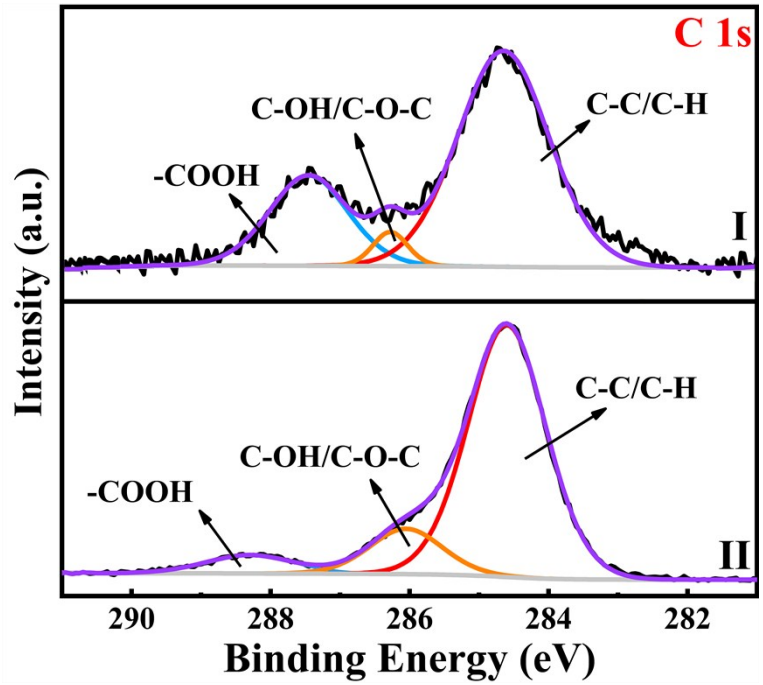


**Fig. S6**. High-resolution C 1s spectra of (I) $T(BC)_4$ and (II) NP-TNTAs.

**Table. S2** Chemical bond species *vs.* BE for different samples.

| *Element* | *CdSe QDs* | *TNTA* | *T(BC)$_4$* | *Chemical Bond Species* |
|---|---|---|---|---|
| **C 1s A** | 284.60 | 284.60 | 284.60 | C-C/C-H |
| **C 1s B** | 286.70 | 286.10 | 286.80 | C-OH/C-O-C[S4] |
| **C 1s C** | 286.90 | 288.20 | 287.80 | Carboxyl (-COO$^-$) [S3] |
| **Cd 3d$_{5/2}$** | 404.61 | N.D. | 404.85 | $Cd^{2+}$ |
| **Cd 3d$_{3/2}$** | 411.28 | N.D. | 411.5 | $Cd^{2+}$ [S5] |
| **Se 3d** | 53.02 | N.D. | 53.12 | $Se^{2-}$ |
| **Ti 2p$_{3/2}$** | N.D. | 458.35 | 458.65 | Anatase (4+) |
| **Ti 2p$_{1/2}$** | N.D. | 463.90 | 464.30 | Anatase (4+) |
| **N 1s** | N.D. | N.D. | 398.40 | Nitride |
| **O 1s** | 530.63 | 531.15 | 531.20 | Ti-OH |

N.D.: Not Detected.

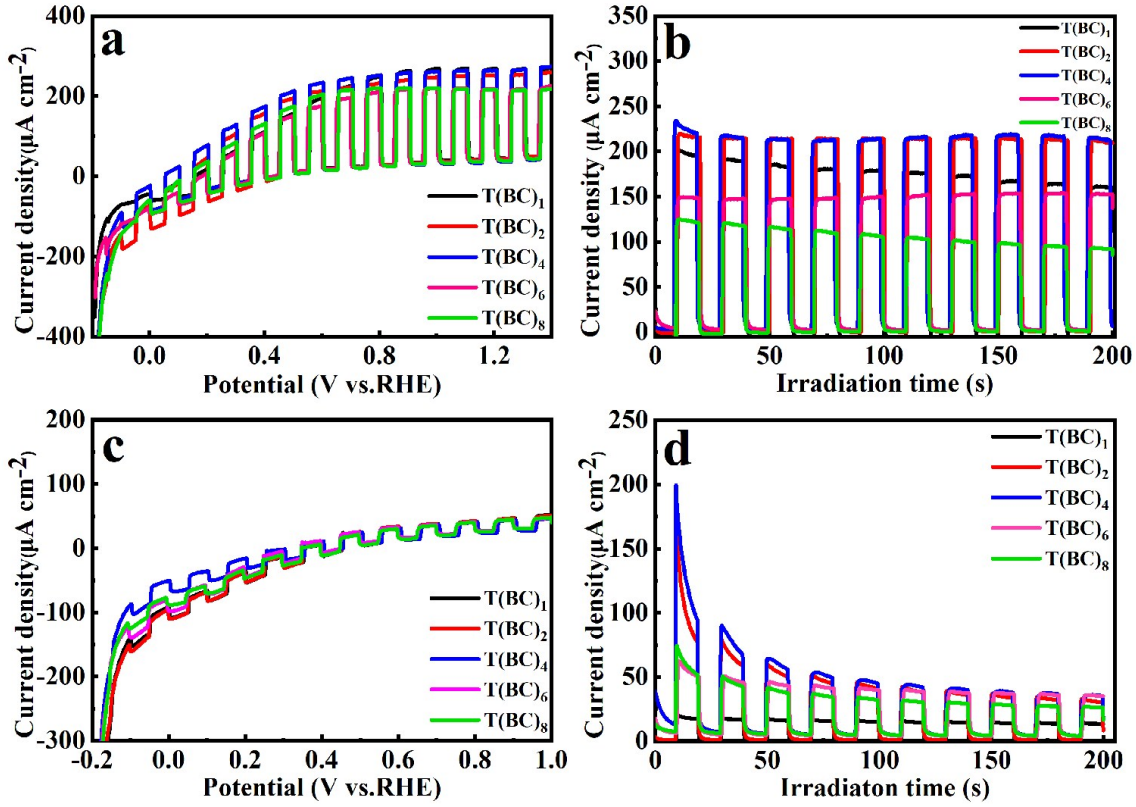


**Fig. S7.** (a & c) LSV results and (b & d) transient photocurrent responses of $T(BC)_n$ (n=1, 2, 4, 6, 8) multilayered heterostructures under simulated solar light (AM1.5G) and visible (λ>420 nm, 0.5 M $Na_2SO_4$, pH=7) light irradiation.

**Note:** $T(BC)_4$ with four assembly bilayer demonstrates the optimal photocurrent density in comparison with other counterparts under both visible (λ>420 nm) and simulated solar (AM 1.5G) light irradiation

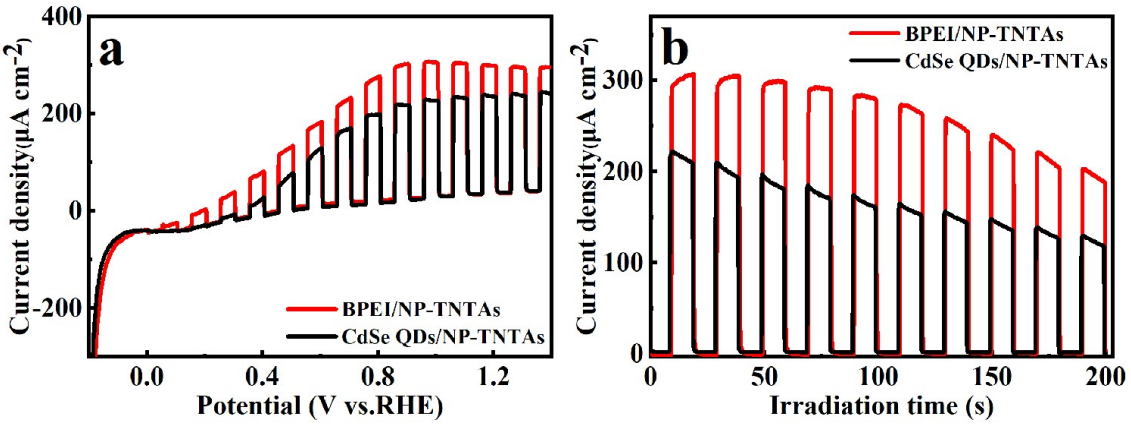


**Fig. S8.** LSV and transient photocurrent results of BPEI/NP-TNTAs and CdSe QDs/NP-TNTAs under simulated solar light (AM1.5G).

**Note:** PEC performances of BPEI/NP-TNTAs and CdSe QDs/NP-TNTAs counterpart which was prepared by directly dipping NP-TNTAs in the BPEI or CdSe QDs aqueous solution for the same time were also probed and the results imply BPEI can also contribute to the photocurrent enhancement as demonstrated by CdSe QDs under simulated solar light irradiation.

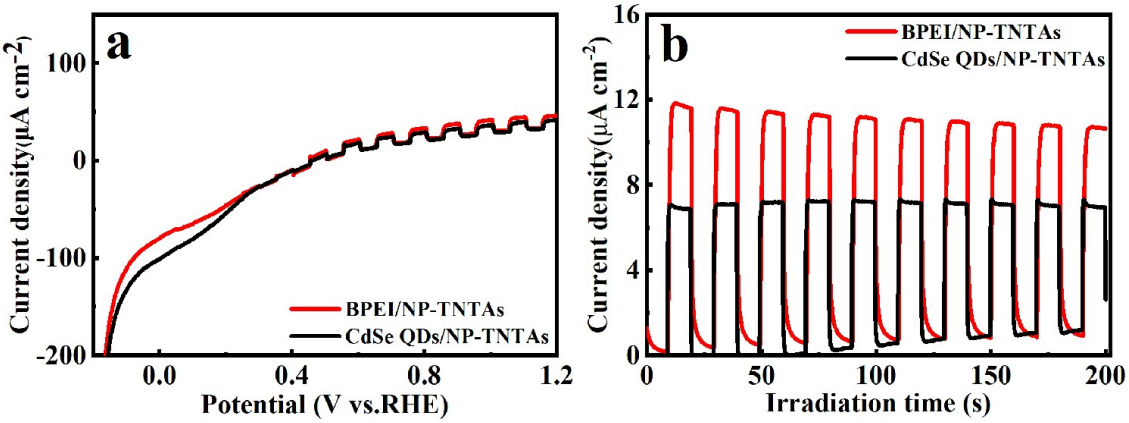


**Fig. S9.** LSV and transient photocurrent results of BPEI/NP-TNTAs and CdSe QDs/NP-TNTAs under visible light irradiation (λ>420 nm).

**Note:** BPEI/NP-TNTAs also exhibits improved photocurrent compared with blank NP-TNTAs under visible light irradiation, once again confirming the crucial role of BPEI and its cooperativity with CdSe QDs in $T(BC)_4$ for photocurrent enchantment.

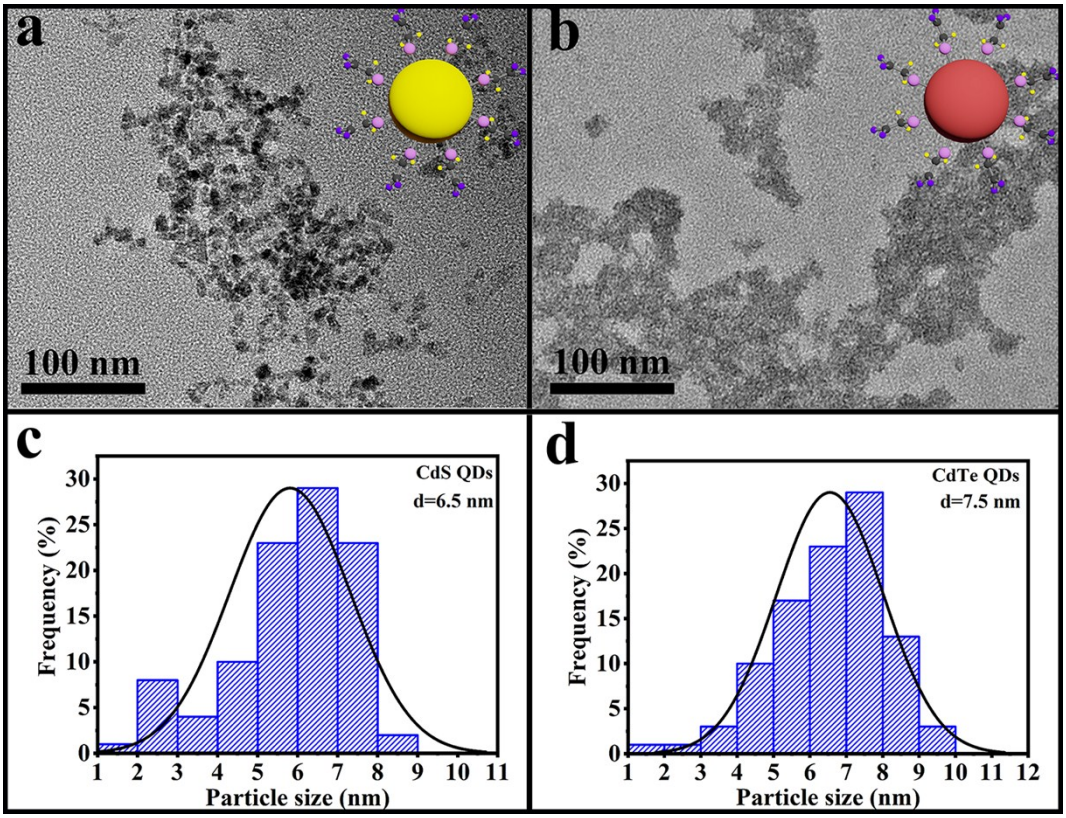


**Fig. S10.** TEM images of (a) CdS@MAA QDs and (b) CdTe@MAA QDs with corresponding (c & d) size distribution histograms.

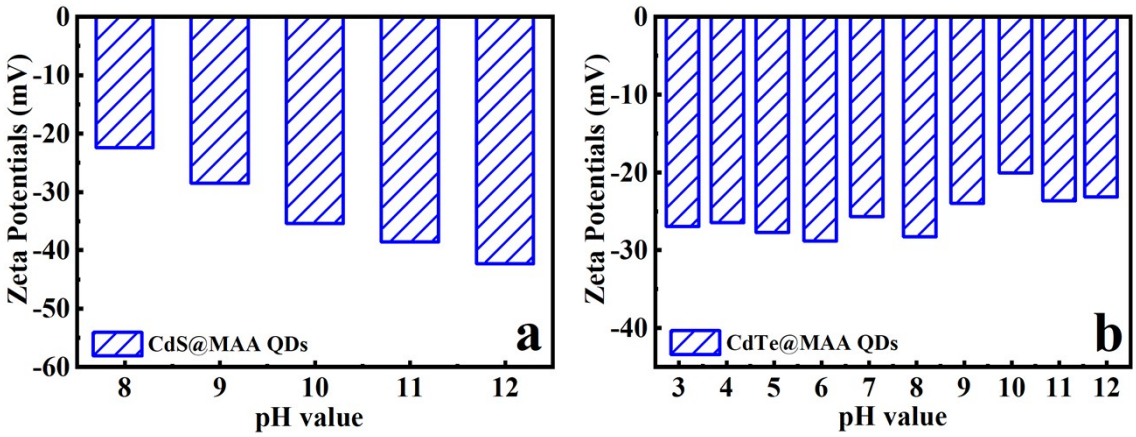


**Fig. S11.** Zeta potentials of (a) CdS@MAA QDs and (b) CdTe@MAA QDs aqueous solutions.

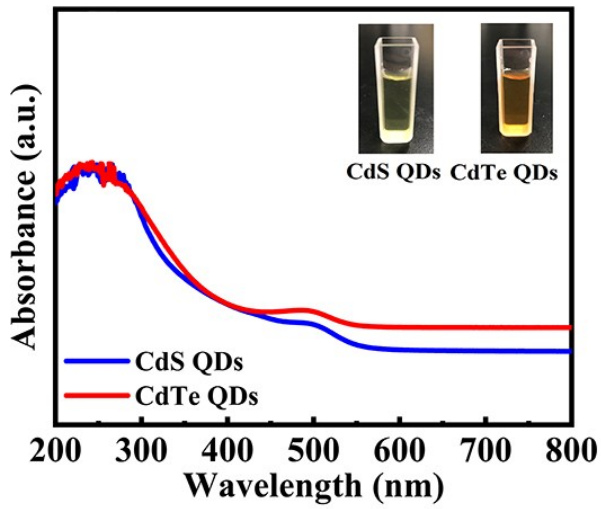


**Fig. S12.** UV-vis absorption spectra of CdS@MAA QDs and CdTe@MAA QDs aqueous solutions with corresponding photographs in the inset.

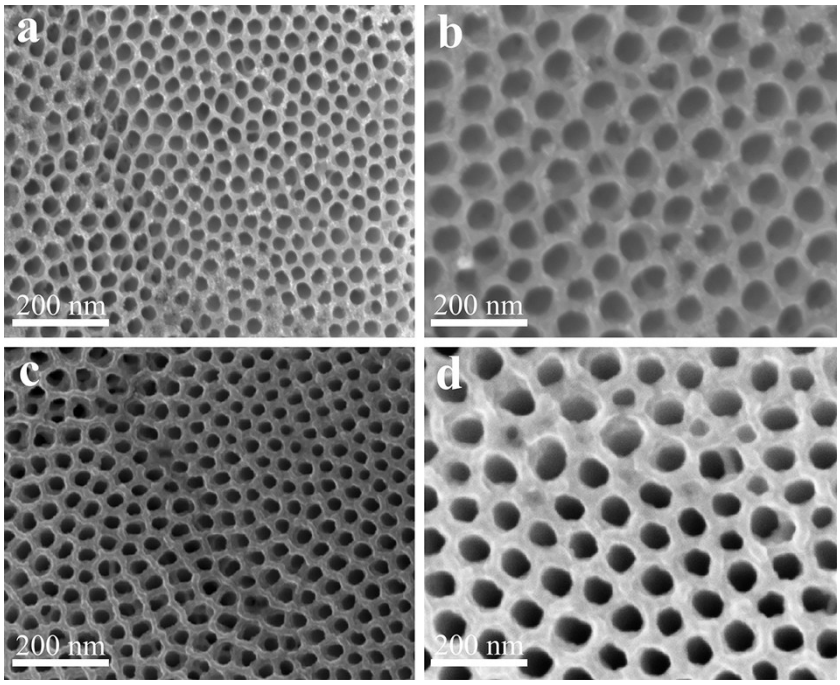


**Fig. S13.** Low and high-magnified FESEM images of (a & b) $T(BS)_4$ and (c & d) $T(BT)_4$ multilayered heterostructures.

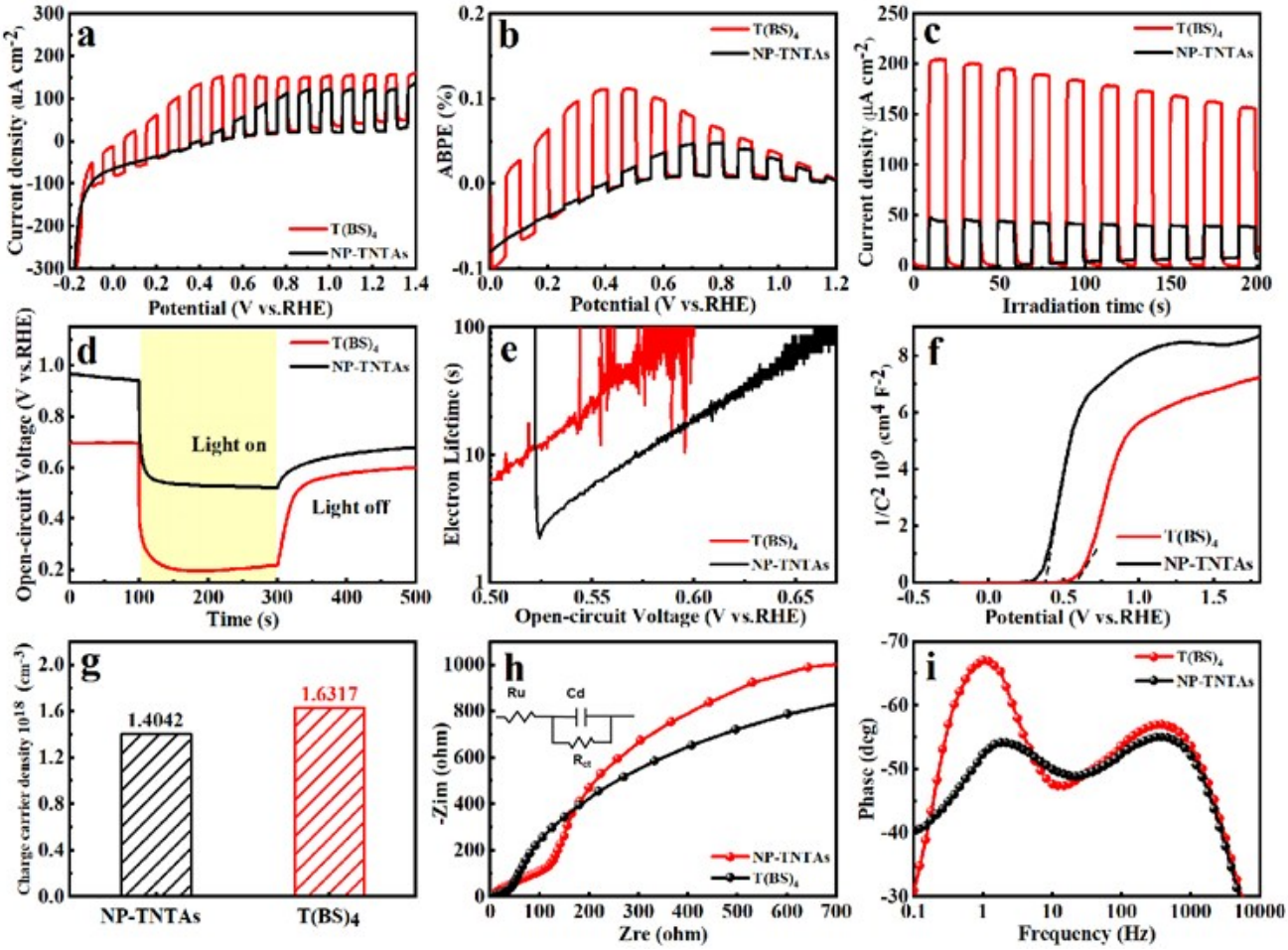


**Fig. S14.** (a & b) LSV curves with ABPE results, (c) transient photocurrent, (d & e) OCVD with electron lifetime, (f & g) Mott-Schottky plots with charge carriers density, (h) EIS curves and (i) Bode phase plots of blank NP-TNTAs and $T(BS)_4$ under simulated solar light irradiation (AM1.5G).

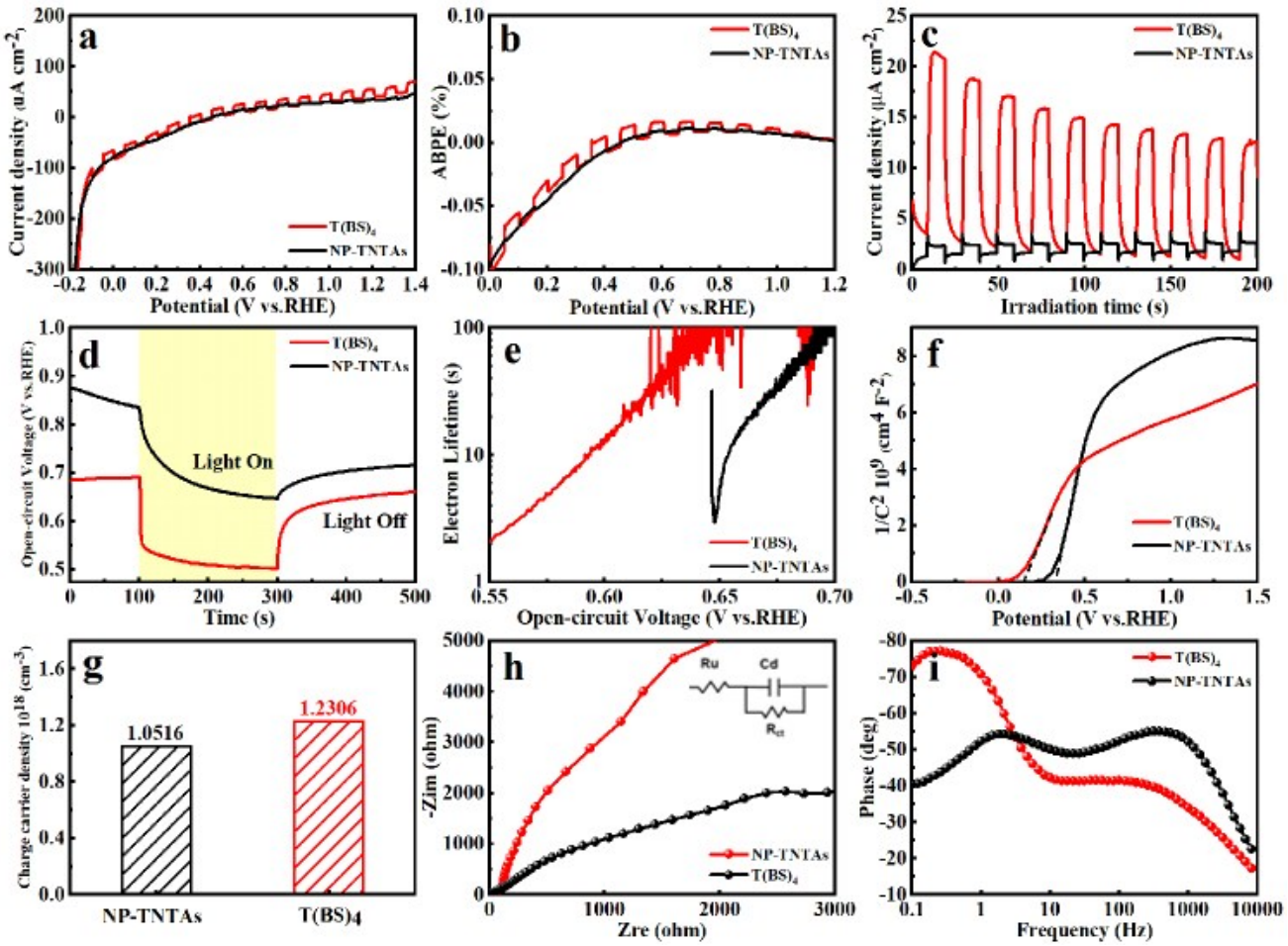


**Fig. S15.** (a & b) LSV curves with ABPE results, (c) transient photocurrent, (d & e) OCVD with electron lifetime, (f & g) Mott-Schottky plots with charge carrier density, (h) EIS curves and (i) Bode phase plots of blank NP-TNTAs and $T(BS)_4$ under visible light irradiation ($\lambda$>420 nm).

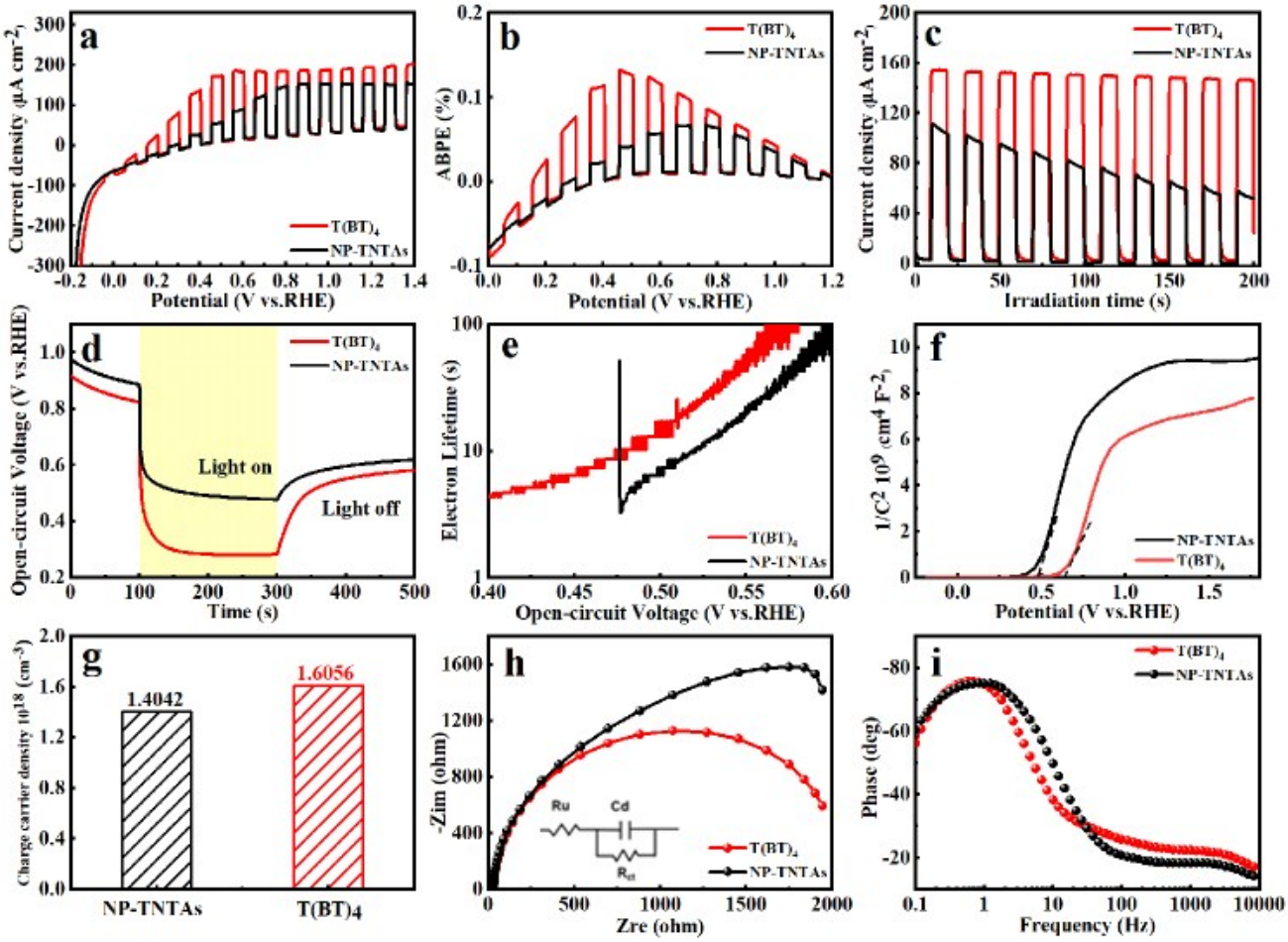


**Fig. S16.** (a & b) LSV curves with ABPE results, (c) transient photocurrent, (d & e) OCVD with electron lifetime, (f & g) Mott-Schottky plots with charge carrier density, (h) EIS curves and (i) Bode phase plots of blank NP-TNTAs and $T(BT)_4$ under simulated solar light irradiation (AM1.5G).

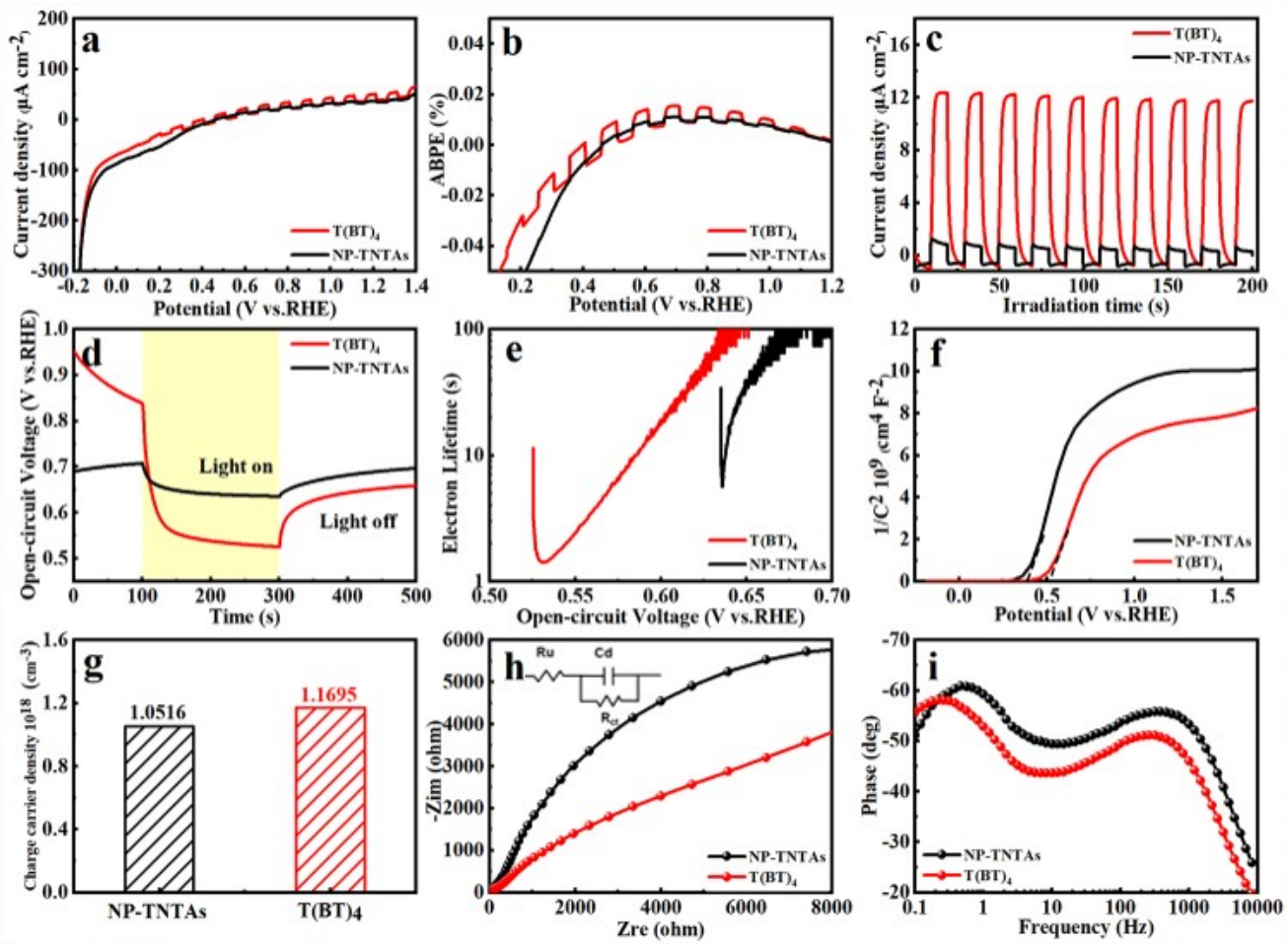


**Fig. S17.** (a & b) LSV curves with ABPE results, (c) transient photocurrent, (d & e) OCVD with electron lifetime, (f & g) Mott-Schottky plots with charge carrier density, (h) EIS curves and (i) Bode phase plots of blank NP-TNTAs and $T(BT)_4$ under visible light irradiation ($\lambda$>420 nm).

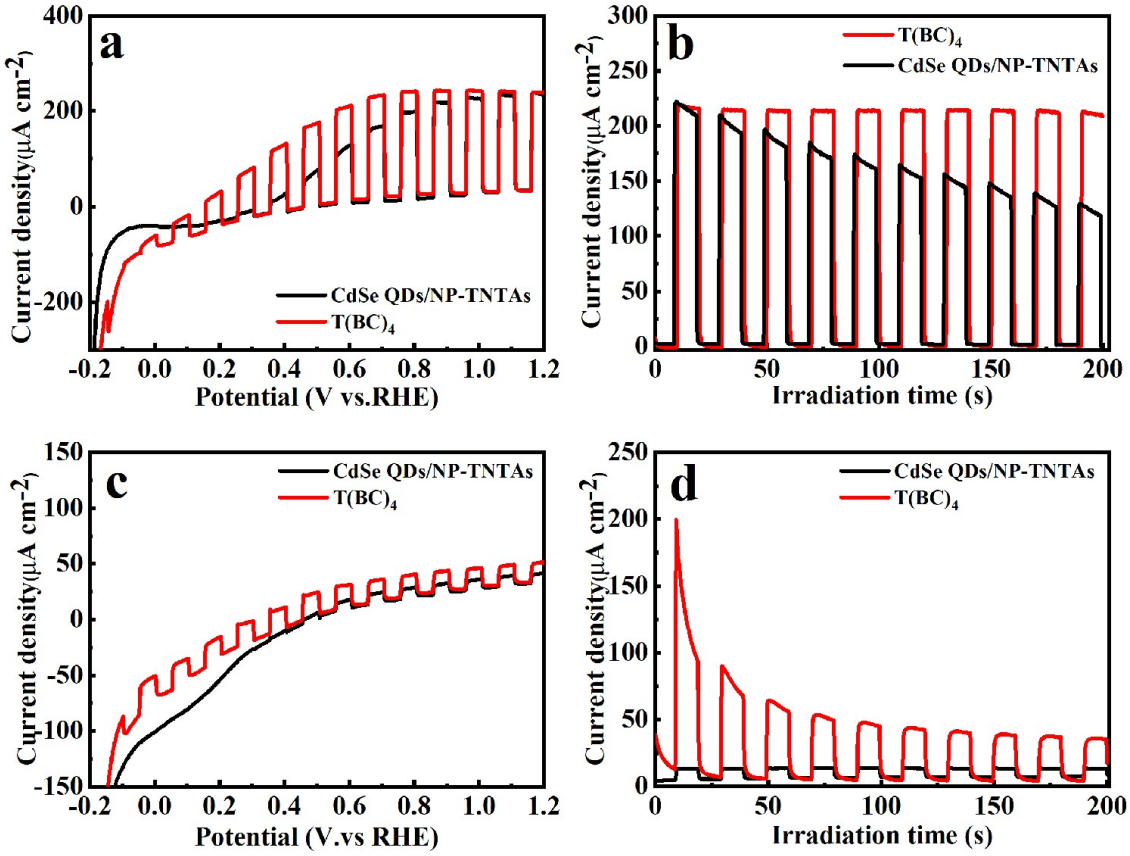


**Fig. S18.** LSV and transient photocurrent results of CdSe QDs/NP-TNTAs and $T(BC)_4$ under (a & b) simulated solar light (AM1.5G) and (c & d) visible light irradiation (λ>420 nm).

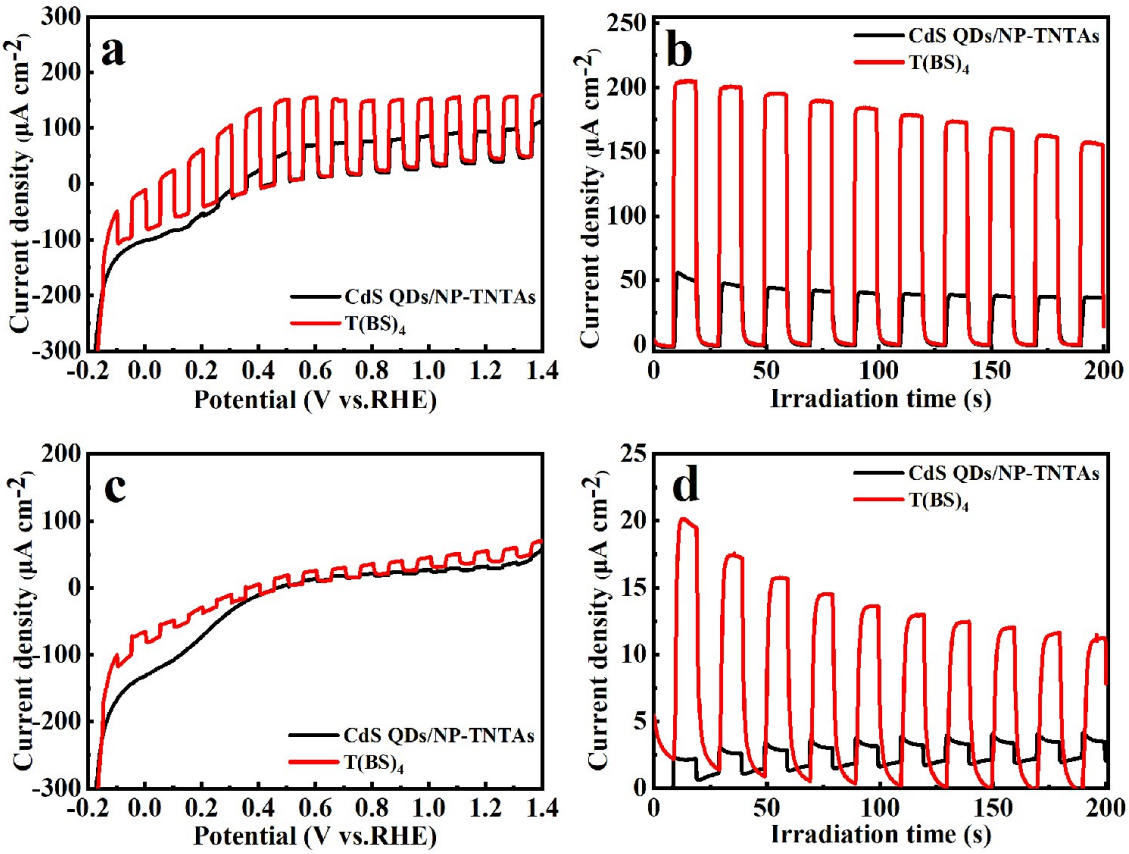


**Fig. S19.** LSV and transient photocurrent results of CdS QDs/NP-TNTAs and $T(BS)_4$ under (a & b) simulated solar light (AM1.5G) and (c & d) visible light irradiation (λ>420 nm).

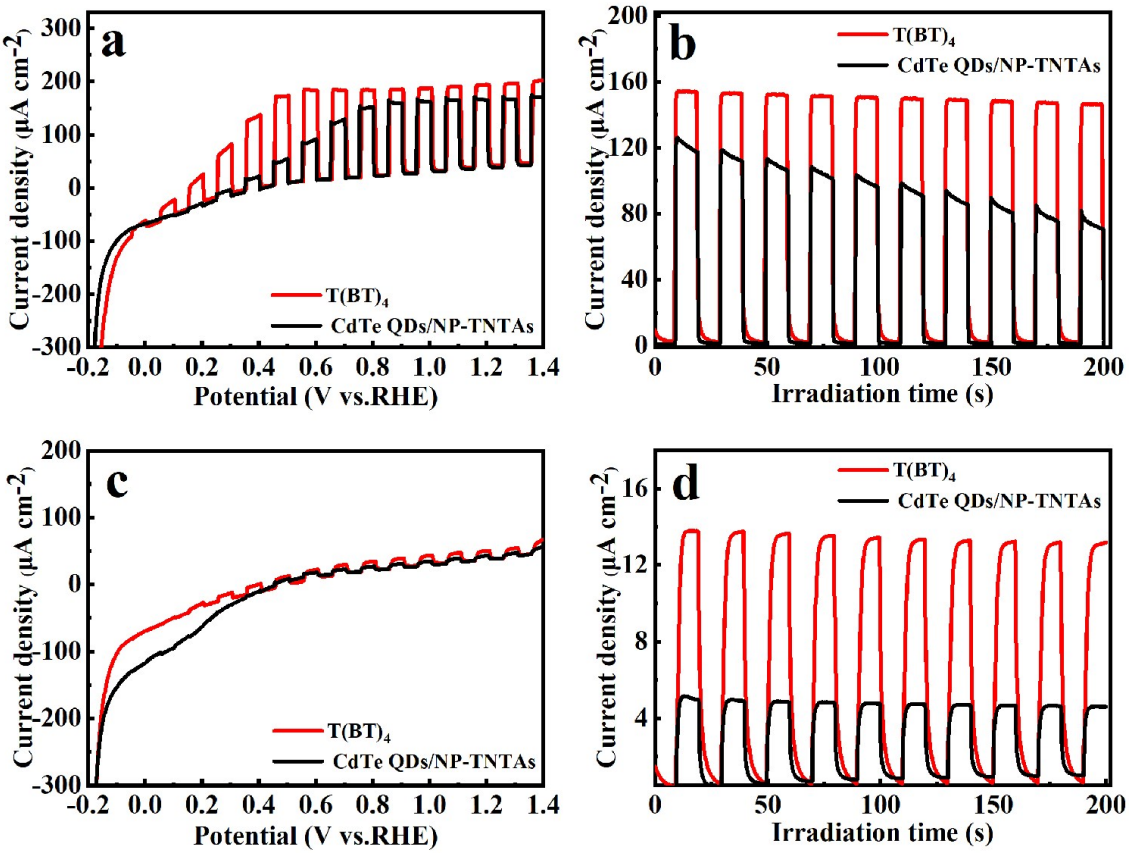


**Fig. S20.** LSV and transient photocurrent results of CdTe QDs/NP-TNTAs and $T(BT)_4$ under (a & b) simulated solar light (AM1.5G) and (c & d) visible light irradiation (λ>420 nm).

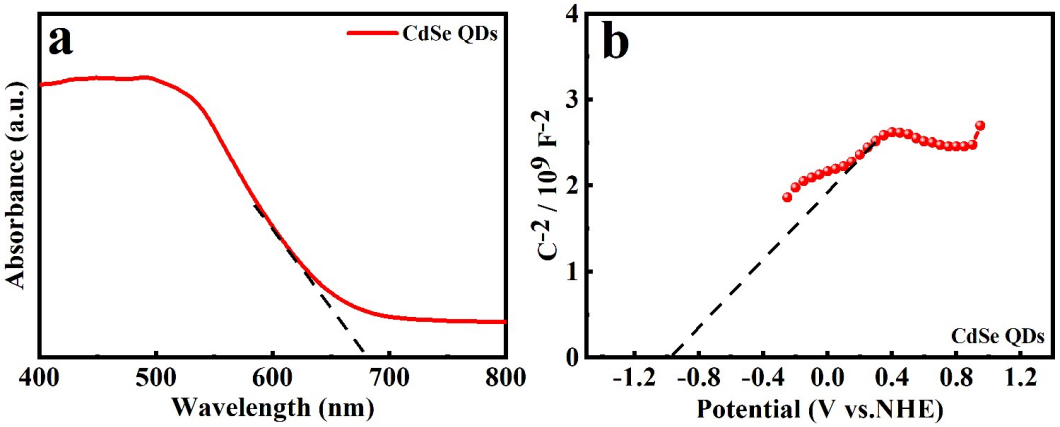


**Fig. S21.** (a) UV-vis adsorption spectrum of CdSe QDs and (b) Mott-Schottky plots of CdSe QDs

**Note:** The transformed plots based on the UV visible light in **Fig. S21 (a)**, by which bandgaps (VB) of the samples can be roughly estimated to be ca. 1.86 eV. And **Fig. S21 (b)** shows the Mott-Schottky plot of CdSe QDs, by which flat band potential (CB) of CdSe QDs was determined to be *ca.* -0.98 V *vs.* Ag/AgCl.

## References


S1. F. -X. Xiao, J. W. Miao and B. Liu, *J. Am. Chem. Soc.*, 2014, **136**, 1559-1569.
S2. M. -H. Huang, X. -C. Dai, T. Li and F. -X. Xiao, *J. Phys.Chem. C*, 2019, **123**, 9721-9734.
S3. H. C. Zeng, F. Xie, K. C. Wong and K. A. R. Mitchell, *Chem. Mater.*, 2002, **14**, 1788-1796.
S4. X. M. Wei and H. C. Zeng, *Chem. Mater.*, 2003, **15**, 433-442.
S5. J. Zhang, J. G. Yu, M. Jaroniec and J. R. Gong, *Nano Lett.*, 2012, **12**, 4584-4589.